Functionalized Carbon Nanotube Thin Films as the pH Sensing Membranes of Extended-Gate Field-Effect Transistors on the Flexible Substrates

Wan-Lin Tsai, Bai-Tao Huang, Kuang-Yu Wang, Yu-Chih Huang, Po-Yu Yang, and Huang-Chung Cheng

***Abstract*—The oxygen-plasma-functionalized carbon nanotube thin films on the flexible substrates as the pH sensing membranes of extended-gate field-effect transistors are proposed for the first time. The carbon nanotubes are ultrasonically sprayed onto the polyimide substrates followed by an oxygen-plasma functionalization. Such oxygen-plasma-treated carbon nanotube thin films (CNTFs) exhibit superior pH sensing characteristics with the sensitivity of 55.7 mV/pH and voltage linearity of 0.9996 in a wide sensing range of pH 1–13. Moreover, the excellent flexibility of carbon nanotube is also demonstrated and the oxygen-plasma-treated CNTFs still maintain the sensitivity of 53.6 mV/pH and voltage linearity of 0.9943 even after five-cycle bending test. These results reveal that the oxygen-plasma-treated CNTFs have great potentials in the practically disposal and wearable biosensor applications.**

***Index Terms*—Biosensors, carbon nanotube (CNT), extended-gate field-effect transistors (EGFETs), flexible substrates.**

I. Introduction

PH sensing is the foundation of numerous biosensors and actively demanded in environment monitoring, biotechnology, analytical chemistry, and medicines [1]–[4]. Since the ion-selective field-effect transistors (ISFETs) was first proposed by Bergveld in 1970 [5], there have been many researches invested in the improvement of sensing characteristics due to the low current sensitivity and instability of ISFETs [6]–[8]. In contrast, extended-gate field-effect transistor (EGFET) was considered as an alternative for the conventional ISFET owing to the lower cost, simpler to package, more insensitive to environment, and better long-term stability [9], [10]. Unlike the integration of an ion selective electrode and a field-effect transistor (FET) in an ISFET, the EGFET is a structure to isolate the FET from the chemical environment, in which a sensing head is extended from the gate electrode through a signal wire. Up to the present, most sensing membranes applied in EGFETs are metal oxides, such as zinc oxide (ZnO) [11], tin oxide (SnO_2) [12], indium tin oxide (ITO) [13], ruthenium oxide RuO_2) [14], and a mixed thin film of vanadium and tungsten oxide (V_2O_5/WO_3) [15], and these metal oxides exhibit well pH sensing characteristics in EGFETs. However, the brittleness of metal oxide might restrict their applications in the flexible and disposal sensors in future.

Recently, carbon-related materials, including graphene [16]–[18] and carbon nanotube (CNT) [19], have been regarded as the promising sensing materials since they possess great electrical properties, outstanding mechanical strength, and good chemical inertness. The epitaxial graphene FET was used in an aqueous environment as a pH sensor in 2008 [17] and then the platform of graphene FET has been mainly fabricated and studied for pH sensing. However, the pH sensing properties of the graphene FETs need to be improved by reason of the low sensitivity to pH levels [18]. Furthermore, the research has still made great efforts to fabricate the low cost, scalable, and reproducible graphene-based pH sensors. On the other hand, the carbon nanotube thin film (CNTF) promises the mass production of highly reliable and practical pH sensing devices. Until now, CNTFs have been mixed with polymer or metal to improve the pH sensing characteristics of the pristine CNTFs. For instance, a carbon felt/carbon nanotube/polyaniline composite as the pH sensing membrane of EGFET [20] and a leaf-like carbon nanotube/nickel composite for the pH-EGFET applications [21] have been reported. Although these proposed composites demonstrated the good pH sensing characteristics, these works did not utilize the CNTFs onto the flexible substrates for the disposal sensor applications in addition to the possibly encountered complex processes and contamination issues.

In this paper, the fully low-temperature and large-area processes for the oxygen-plasma-functionalized CNTFs on the polyimide (PI) substrates as the sensing membranes of EGFETs were thereby proposed. The CNTs were ultrasonically sprayed onto the PI substrates and subsequently treated by an oxygen-plasma functionalization. Then, the pH sensing characteristics and reliability test of these oxygen-plasma-treated CNTFs on the PI substrates were systematically discussed.

II. Device Structure and Fabrication

A homogeneous multiwalled CNT (MWCNT) solution could be obtained after an acid treatment as described in our earlier study [22]. At first, the MWCNT solution was sprayed onto the

Manuscript received November 12, 2013; revised March 5, 2014; accepted April 14, 2014. Date of publication April 24, 2014; date of current version July 2, 2014. This work was supported by the National Science Council of Taiwan under Contract NSC 101-2221-E-009-077-MY3. The review of this paper was arranged by Associate Editor M. M. De Souza.

W.-L. Tsai, B.-T. Huang, K.-Y. Wang, Y.-C. Huang, and H.-C. Cheng are with the Department of Electronics Engineering and the Institute of Electronics, National Chiao Tung University, Hsinchu 300, Taiwan (e-mail: nctuwltsai@gmail.com; mystoryoursong@yahoo.com.tw; h063910333@yahoo.com.tw; antares.ee97g@nctu.edu.tw; hccheng536@mail.nctu.edu.tw).

P.-Y. Yang is with the Taiwan Semiconductor Manufacturing Company, Hsinchu 300, Taiwan (e-mail: youngboyalan@yahoo.com.tw).

Color versions of one or more of the figures in this paper are available online at http://ieeexplore.ieee.org.

Digital Object Identifier 10.1109/TNANO.2014.2318710

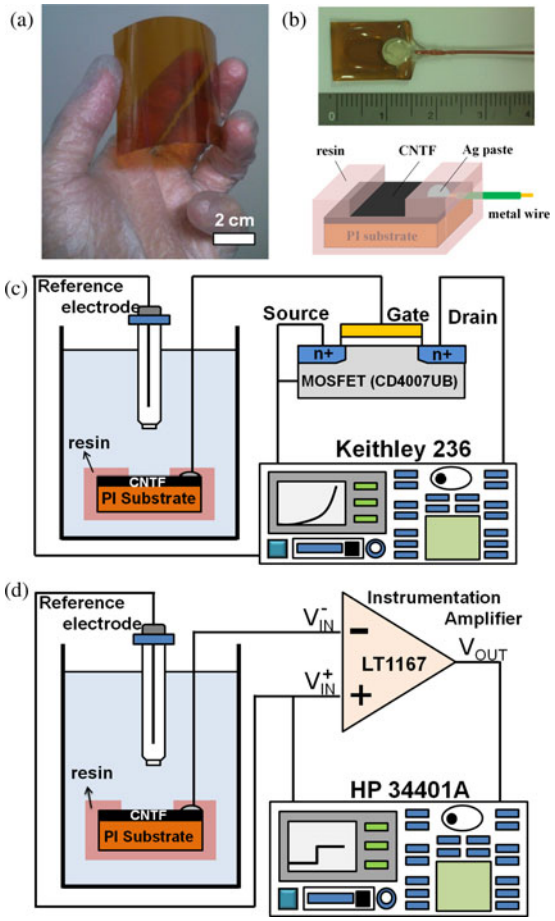

Fig. 1. (a) Picture of as-sprayed CNTF on a PI substrate. (b) The picture and schematic diagram of the sensing head structure. (c) Schematic diagram of the I–V measurement system for the pH-EGFET sensors. (d) Schematic diagram of the V-t measurement system for the pH-EGFET sensors.

PI substrates at 180 °C to form the CNTFs. A PI sheet with an area of 36 square centimeters after the MWCNTs spraying exhibited the flexible appearance, as shown in Fig. 1(a). Subsequently, some as-sprayed CNTFs were treated with the oxygen plasma generated in the high-density-plasma (HDP) reactive ion etching system at 10^{-2} torr with the oxygen flow rate of 20 sccm under the inductively coupled plasma (ICP) power of 100 W and bias power from 20 to 60 W for 90 s. Finally, both the as-sprayed CNTFs and oxygen-plasma-treated ones were bonded to the metal wires with the silver paste and baked at 150 °C for 30 min. All these samples were then encapsulated with the ethylene vinyl acetate copolymer resin with a sensing window defined as $4 \times 4\,\text{mm}^2$ to form the sensing heads of the EGFETs. Here, 120 devices had been fabricated, of which 30 devices were made from as-sprayed CNTFs and the last 90 devices were equally made from the plasma-treated CNTFs with power of 20, 40, and 60 W, respectively. Fig. 1(b) exhibits the picture and schematic diagram of the sensing head structure. A Keithley 236 semiconductor parameter analyzer was utilized to measure the current–voltage $(I$–$V)$ characteristics of the pH-EGFET sensors, connected to the gate of commercial standard MOSFET device (CD4007UB), in pH = 1, 3, 5, 7, 9, 11, and

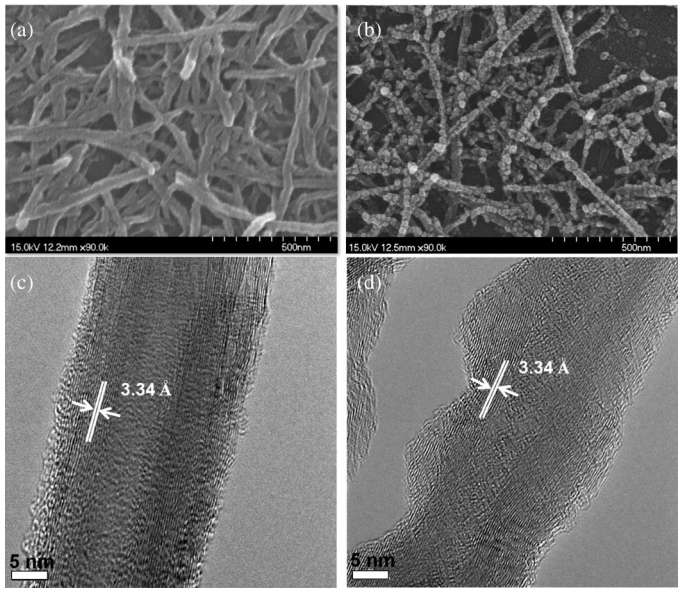

Fig. 2. (a) SEM image of as-sprayed CNTF. (b) SEM image of oxygen-plasma-treated CNTF with bias power of 40 W for 90 s. (c) TEM image of as-sprayed CNT with a lattice constant of 3.34 Å. (d) TEM image of oxygen-plasma-treated CNT with a lattice constant of 3.34 Å.

13 phosphate buffer solutions (PBSs), as shown in Fig. 1(c). Moreover, the measurement system consisted of a digital multimeter (HP 34401A) and a commercial instrument amplifier (IC LT1167) was applied to analyze the voltage–time characteristics of the pH-EGFET sensors, as shown in Fig. 1(d).

III. Results and Discussion

The field-emission scanning electron microscopy (FE-SEM) images of the morphological variations of CNTFs on the PI substrates before and after the plasma treatment are shown in Figs. 2(a) and (b), respectively. The as-sprayed CNTs, i.e., the ones before the plasma treatment, can be recognized individually and distributed arbitrarily with smooth surface, as shown in Fig. 2(a). After the oxygen–plasma treatment with the bias power of 40 W for 90 s, the CNTs significantly change from smooth to much rougher surface, as exhibited in Fig. 2(b). To further realize the effect of the plasma treatment on the structure of CNT, the high-resolution transmission electron microscopy (TEM) is applied to further analyze the CNTs before and after the plasma process. Fig. 2(c) obviously indicates a regular and coaxial multiwalled CNT with a lattice constant of 3.34 Å for the sample before the plasma treatment. In contrast, the MWCNT after the plasma treatment shows the zig-zag surface very different from the one before plasma treatment although the lattice constant is still 3.34 Å for the inner-layered sidewalls, as shown in Fig. 2(d). The formed zig-zag surface is attributed to some concave holes created on the MWCNTs via the oxygen–plasma treatment. These concave holes have been initially formed from the weak points of sidewalls, such as the Stone–Wales defects [23], and enlarged with the increasing of bias power. Moreover, the other side of the MWCNT which is away from the plasma bombardment direction appears

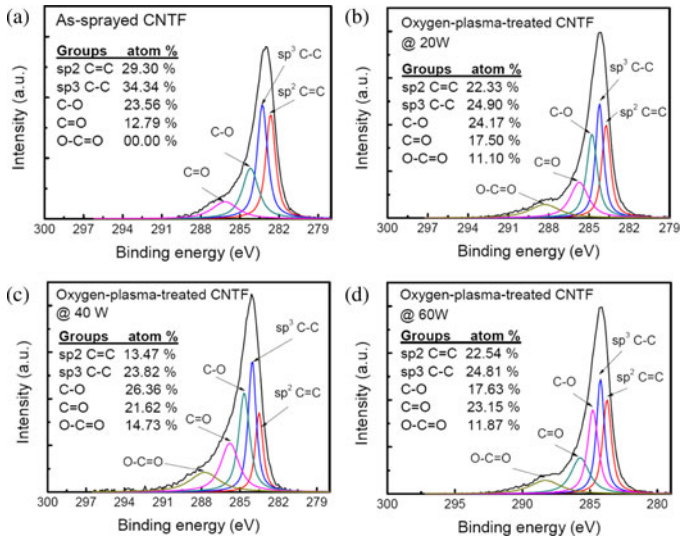

Fig. 3. XPS C 1-s spectra of (a) as-sprayed and oxygen-plasma-treated CNTFs with bias power of (b) 20 W, (c) 40 W, and (d) 60 W can be deconvolved into five Gaussian peaks: 284.1 ± 0.2 eV, 285.1 ± 0.2 eV, 286.2 ± 0.2 eV, 287.2 ± 0.2 eV, and 288.9 ± 0.2 eV in sequence.

relatively smooth with respect to the directly bombarded surface of MWCNT. It is believed that the plasmas are accelerated to bombard the surface of the MWCNT but the other sidewall survives from the surface plasma bombardment.

The X-ray photoelectron spectroscopy (XPS) is performed to examine the decorated functional groups on the CNTs after the plasma treatment, as shown in Fig. 3. The XPS C 1s spectra of the CNTFs could be deconvolved into five Gaussian peaks [24]. The main peak at 284.1 ± 0.2 eV is attributed to the sp^2-hybridized graphite-like carbon atoms (C=C). The peak at 285.1 ± 0.2 eV corresponds to the sp^3-hybridized carbon atoms (C–C). Other peaks at 286.2 ± 0.2 eV, 287.2 ± 0.2 eV, and 288.9 ± 0.2 eV are considered to originate from the carbon atoms bound to one oxygen atom with a single bond, one oxygen atom with double bonds, and two oxygen atoms, accordingly. It is obvious that the quantity of sp^2 C=C bonds decreases but those of the oxygen-containing groups, such as C–O, C=O, and O–C=O bonds, increase as the CNTFs were under the conditions from without to with the plasma treatments of 20 W until 40 W. However, CNTs will be damaged to even cause the decomposition after the plasma treatment with the bias power of 60 W. Therefore, the quantities of the oxygen-containing groups decrease instead as the bias power is over 60 W. These consequences indicate that the oxygen-plasma treatment is an efficient way to functionalize the CNTs which causes a large number of C=C bonds to be substituted with the oxygen-containing groups.

The transfer characteristics (drain current versus reference electrode voltage, $I_{\rm DS} - V_{\rm REF}$) in the linear region for the pH-EGFET sensors with the as-sprayed CNTFs and oxygen-plasma-treated CNTFs at the bias power of 40 W are shown in Figs. 4(a) and (b), respectively, for the $V_{\rm DS}$ fixed at 0.2 V and $V_{\rm REF}$ varied from 0 to 4 V. The $I_{\rm DS} - V_{\rm REF}$ curves exhibit a threshold voltages shift from left to right with the decreasing of the hydrogen ion concentration in the range of pH 1–13. The

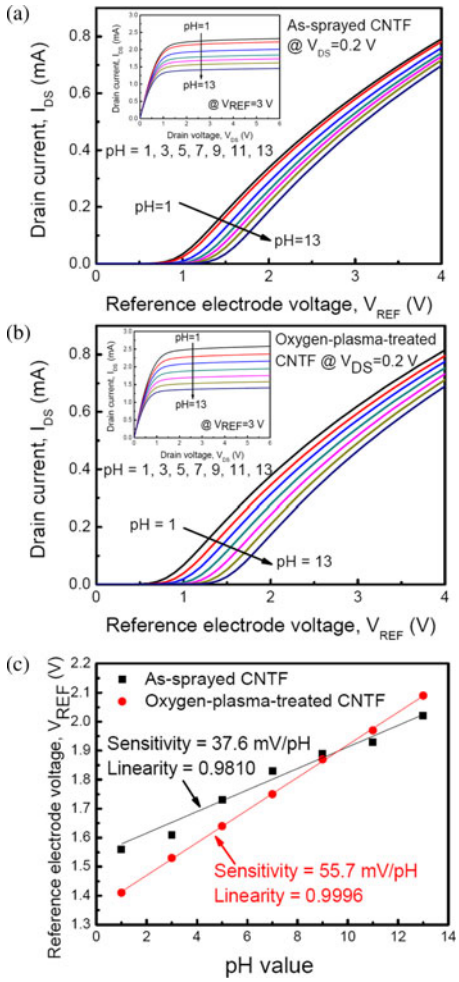

Fig. 4. (a) Transfer characteristics of the pH-EGFET sensors in the linear region for as-sprayed CNTFs on the flexible PI substrates. The corresponding curves in the saturation region with $V_{\rm REF} = 3\,V$ are also depicted in the inset of (a). (b) The transfer characteristics of the pH-EGFET sensors in the linear region for oxygen-plasma-treated CNTFs on the flexible PI substrates with bias power of 40 W for 90 s. The corresponding curves in the saturation region with $V_{\rm REF} = 3\,V$ are also depicted in the inset of (c). (d) The extracted pH voltage sensitivity and linearity for the as-sprayed CNTFs and oxygen-plasma-treated ones.

corresponding $I_{\rm DS} - V_{\rm DS}$ curves in the saturation region with $V_{\rm REF} = 3\,V$ are also depicted in the insets, correspondingly. The voltage sensitivity for pH-EGFET sensors is calculated from the slopes of the $V_{\rm REF}$, defined at the fixed $I_{\rm DS}$ of 0.2 mA and $V_{\rm DS}$ of 0.2 V, against the pH values, as depicted in Fig. 4(c). Consequently, the voltage sensitivities of the as-sprayed CNTFs and oxygen-plasma-treated CNTFs are 37.6 and 55.7 mV/pH, accordingly. Furthermore, the extracted pH voltage linearity for the oxygen-plasma-treated CNTFs is 0.9996 which is significantly better than 0.9810 for the as-sprayed ones. Based on the Nernst equation [25], the theoretical value of voltage sensitivity for the pH sensing is about 59.1 mV/pH. In other words, our experimental results of 55.7 mV/pH for the oxygen-plasma-treated CNTFs present a much better response with respect to the as-sprayed CNTFs. Moreover, as compared to other pH sensing platforms, such as Si_3N_4-gated ISFET [7] and SiO_2-gated ISFET [8], the oxygen-plasma-treated CNTFs demonstrate the

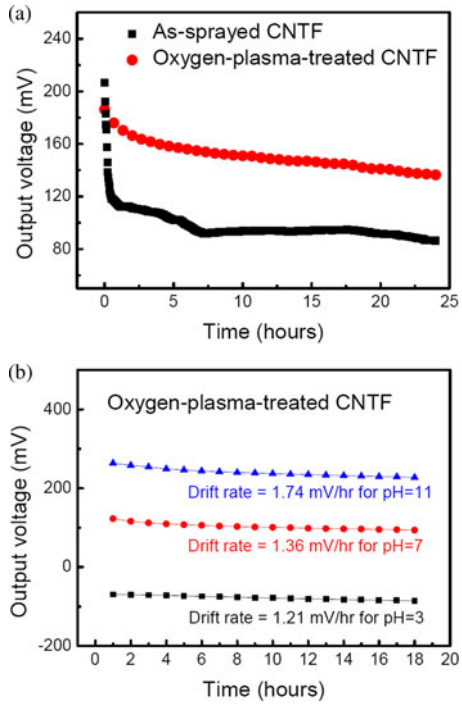

Fig. 5. (a) Long-term stability of as-sprayed CNTFs and oxygen-plasma-treated ones on the flexible PI substrates with bias power of 40 W for 90 s in pH 7 buffer solutions. (b) The chemical drifts of oxygen-plasma-treated CNTFs on the flexible PI substrates in pH 3, pH 7, and pH 11 buffer solutions.

higher pH voltage sensitivity and larger linearity which can accurately respond to the ions of interest in different pH levels.

The voltage drift is a nonideal effect of EGFET, which is related to the adsorption and desorption of the mobile ions on the surface of sensing membrane at varied buffer solutions [26]. As the pH-EGFET is immersed to the PBS solution, the surface of the sensing membrane is subject to hydration, or the permeation of water molecule and ions into the sensing membrane, resulting in a slow monotonic change in voltage which may last over several hours. Therefore, the long-term stability of as-sprayed CNTFs and oxygen-plasma-treated CNTFs in pH 7 buffer solution is shown in Fig. 5(a). For the pH-EGFET sensors of the oxygen-plasma-treated CNTFs, the output voltages decrease slightly as the time increases, and this relatively small variation amount with respect to the as-sprayed ones presents that the oxygen-plasma-treated CNTFs are the more stable sensing films for the pH-EGFETs. Moreover, the chemical drifts of oxygen-plasma-treated CNTFs in pH 3, pH 7, and pH 11 buffer solutions are shown in Fig. 5(b), respectively. The drift rate of the pH-sensitive device is defined as the slope of the output voltage from 5 to 12 h against the measurement time [27]. The drift rates are 1.21 mV/pH for pH 3, 1.36 mV/pH for pH 7, and 1.74 mV/pH for pH 11, accordingly. Obviously, the drift rates increase while the pH value increases which are the similar trend with the other reported literatures [28].

Since the CNT is the strongest and stiffest material resulted from the covalent sp^2 bonds formed between the individual carbon atoms ever discovered [29], a bending test is then taken to examine the reliability of CNTFs in the pH sensing of EGFET

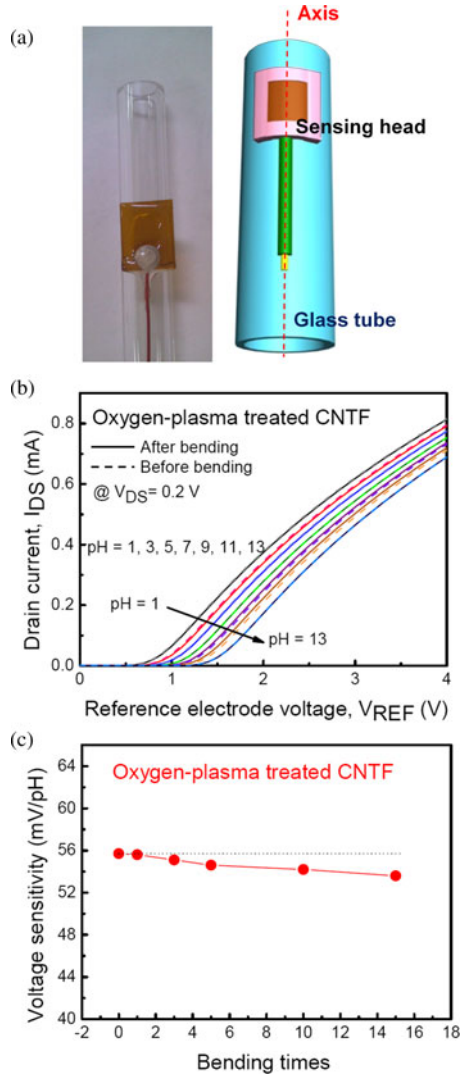

Fig. 6. (a) Picture and schematic diagram of the bending test. (b) The transfer characteristics of the pH-EGFET sensors in the linear region for oxygen-plasma-treated CNTFs on the flexible PI substrates before (dashed lines) and after (solid lines) five-cycle bending test. (c) The decay of voltage sensitivity with increasing bending times for oxygen-plasma-treated CNTFs on the flexible PI substrates.

sensors. Thirty pH-EGFETs fabricated by the plasma-treated CNTFs with bias power of 40 W for 90 s were tested. The sensing heads are faced up on a glass tube with an outer diameter of 1 cm and then bent until they perfectly fit with the curvature of the glass tube, as shown in Fig. 6(a) for the picture and the corresponding schematic diagram. To ensure the bending curvature to be the same in each bending test, the axis of the sensing head is aligned with that of the glass tube. Each pH-EGFET was tested in five cycles and 34-times bending in total, i.e., bent 1 time and measured (first cycle), bent three times and measured (second cycle), bent five times and measured (third cycle), bent ten times and measured (fourth cycle), and then bent 15 times and measured (fifth cycle). As shown in the solid lines of Fig. 6(b), the oxygen-plasma-treated CNTFs exhibit the similar transfer characteristics to those CNTFs before bending, as shown in the dashed lines of Fig. 6(b), in the linear region for the V_{DS} fixed at 0.2 V and V_{REF} varied from 0 to 4 V after

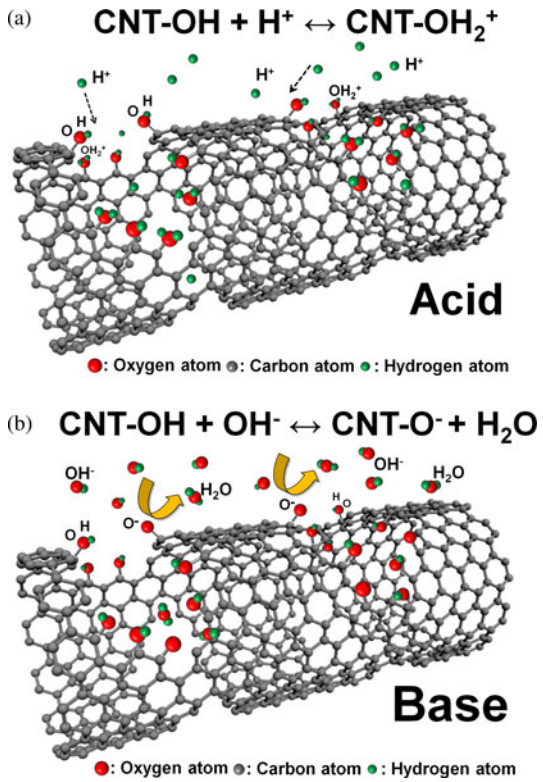

Fig. 7. Schematic diagram for the sensing mechanism of CNTF in (a) acid and (b) base.

five-cycle bending test. Fig. 6(c) shows the voltage sensitivity against bending times for the oxygen-plasma-treated CNTFs. It is evident that the oxygen-plasma-treated CNTFs still sustain the outstanding voltage sensitivity of 53.6 mV/pH and the high voltage linearity of 0.9943 even after five-cycle bending test. The slight decreasing rate of the voltage sensitivity with the increasing bending times demonstrates the superior pH-sensing characteristics of the oxygen-plasma-treated CNTFs for the flexible pH-EGFET sensors.

A sensing mechanism for the oxygen-plasma-treated CNTF is therefore proposed. While the CNTFs immersed in the PBSs, the oxygen-containing groups transfer to hydroxyl bonds, i.e., C-OH, and the interface between the CNTF and solution will build up a layer of capacitance. Under the thermodynamic status, the reaction of H^+ combination in acid and dissociation in base can be illustrated in Fig. 7. Based on the site-binding model, the threshold voltage $V_{\mathrm{T(EGFET)}}$ of pH-EGFET sensors could be expressed in the following equation [30], [31]:

$$V_{\mathrm{T(EGFET)}} = V_{\mathrm{T(MOSFET)}} - \frac{\Phi_M}{q} + E_{\mathrm{REF}} + \chi_{\mathrm{sol}} - \varphi \quad (1)$$

where $V_{\mathrm{T(MOSFET)}}$ is the threshold voltage of the MOSFET, Φ_M is the work function of the metal gate (reference electrode, Ag/AgCl) relative to vacuum, E_{REF} is the potential of the reference electrode, χ_{sol} is the surface dipole potential of the buffer solution, and φ is the surface potential at the interface of solution and CNTF. Therefore, H^+ ions combine with the hydroxyl bonds on the surface of CNTs in acid, as shown in Fig. 7(a), resulting in a lower $V_{\mathrm{T(EGFET)}}$ for the higher surface potential. Contrarily, surface potential is lower in the base because H atoms are dissociated from hydroxyl bonds by combining with OH^- ions to form H_2O, as shown in Fig. 7(b), and then the threshold voltage $V_{\mathrm{T(EGFET)}}$ will shift to the right with increasing pH. According to the site-binding model, a parameter of β can reflect the chemical sensitivity of the sensing film and is given by [32]

$$\beta = \frac{2q^2 N_s \left(\frac{K_b}{K_a}\right)^{1/2}}{kTC_{\mathrm{DL}}} \quad (2)$$

where q is the electronic charge, N_s is the total number of sensing sites per unit area, K_a and K_b are the acid and base equilibrium constants, κ is the Boltzmann's constant, T is the temperature of the system, and C_{DL} is the double-layer capacitance at the interface, which is derived by Gouy–Chapman–Stern model [33]. From the equation of β, it indicates that there are higher sensitivity and larger linearity of the sensing films when the value of β increases and β is proportion to the total number of sensing sites per unit area N_s. Therefore, a large number of oxygen-containing groups are decorated on the surfaces of CNTs after the oxygen-plasma treatment, resulting in a higher value of N_s, and these functional groups act as the sensing sites and accurately respond to the ions of interest in different pH levels. Consequently, the CNTFs after the oxygen-plasma treatment demonstrate the remarkable sensing characteristics as the sensing membranes of the flexible pH-EGFET sensors.

IV. Conclusion

The oxygen-plasma-treated CNTFs on the PI substrates have been successfully demonstrated to achieve the superior sensing characteristics of the flexible pH-EGFET sensors. Oxygen-plasma functionalization can decorate sufficient sensing sites on the surfaces of CNTs, therefore, such oxygen-plasma-treated CNTFs exhibit the pH sensing characteristics with the sensitivity of 55.7 mV/pH and voltage linearity of 0.9996 in a wide sensing range of pH 1–13. Moreover, the oxygen-plasma-treated CNTFs on PI substrates still sustain the sensitivity of 53.6 mV/pH and voltage linearity of 0.9943 even after five-cycle bending test. These results indicate that oxygen-plasma-treated CNTFs on the PI substrates have the great potentials in the applications for the flexible disposal and wearable biosensors.

References

[1] A. Jang, Z. Zou, K. K. Lee, C. H. Ahn, and P. L. Bishop, "State-of-the-art lab chip sensors for environmental water monitoring," *Meas. Sci. Technol.*, vol. 22, pp. 032001–032019, Jan. 2011.

[2] K. Olga, A. Khalil, G. Edric, and A. Arousian, "Review paper: Materials and techniques for in vivo pH monitoring," *IEEE Sensor J.*, vol. 8, pp. 20–28, May 2008.

[3] W. Vonau and U. Guth, "pH monitoring: A review," *J. Solid State Electrochem.*, vol. 10, pp. 746–752, Apr. 2006.

[4] A. K. Terry, S. George, and P. Etana, "Molecular aspects of bacterial pH sensing and homeostasis," *Nature Rev. Microbiol.*, vol. 9, pp. 330–343, May 2011.

[5] P. Bergveld, "Development of an ion sensitive solid-state device for neurophysiological measurement," *IEEE Trans. Biomed. Eng.*, vol. BME-17, no. 1, pp. 70–71, Jan. 1970.

[6] L. Bousse, D. Hafeman, and N. Tran, "Time-dependence of the chemical response of silicon nitride surfaces," *Sens. Actuators B*, vol. 1, pp. 361–367, Jan. 1990.
[7] V. K. Khanna, "Remedial and adaptive solutions of ISFET non-ideal behavior," *Sens. Rev.*, vol. 33, pp. 228–237, 2013.
[8] S. C. Chen, Y. K. Su, and J. S. Tzeng, "The fabrication and characterisation of ion-sensitive field-effect transistors with a silicon dioxide gate," *J. Phys. D: Appl. Phys.*, vol. 19, pp. 1951–1956, Apr. 1986.
[9] J. C. Chou, J. L. Chiang, and C. L. Wu, "pH and procaine characteristics of the extended gate field effect transistor based on ITO glass," *Jpn. J. Appl. Phys.*, vol. 44, pp. 4838–4842, Jul. 2005.
[10] J. L. Chiang, J. C. Chou, and Y. C. Chen, "Study of pH-ISFET and EnFET for biosensor applications," *J. Med. Bio. Eng.*, vol. 21, pp. 135–146, Jul. 2001.
[11] P. D. Batista and M. Mulato, "ZnO extended-gate field-effect transistors as pH sensors," *Appl. Phys. Lett.*, vol. 87, pp. 143508-1–143508-3, Oct. 2005.
[12] H. H. Li, W. S. Dai, J. C. Chou, and H. C. Cheng, "An extended-gate field-effect transistor with low-temperature hydrothermally synthesized SnO_2 nanorods as pH sensor," *IEEE Electron Device Lett.*, vol. 33, no. 10, pp. 1495–1497, Oct. 2012.
[13] J. L. Chiang, S. S. Jhan, S. C. Hsieh, and A. L. Huang, "Hydrogen ion sensors based on indium tin oxide thin film using radio frequency sputtering system," *Thin Solid Films*, vol. 517, pp. 4805–4809, Mar. 2009.
[14] J. C. Chou and D. J. Tzeng, "Study on the characteristics of the ruthenium oxide pH electrode," *Rare Metal Mater. Eng.*, vol. 35, pp. 256–258, Jul. 2006.
[15] E. J. Guidelli, E. M. Guerra, and M. Mulato, "V_2O_5/WO_3 mixed oxide films as pH-EGFET sensor: Sequential re-usage and fabrication volume analysis," *J. Solid State Sci. Technol.*, vol. 1, pp. 39–44, Aug. 2012.
[16] Z. Cheng, Q. Li, Z. Li, Q. Zhou, and Y. Fang, "Suspended graphene sensors with improved signal and reduced noise," *Nano Lett.*, vol. 10, pp. 1864–1868, Apr. 2010.
[17] P. K. Ang, W. Chen, A. T. S. Wee, and K. P. Loh, "Solution-gated epitaxial graphene as pH sensor," *J. Amer. Chem. Soc.*, vol. 130, pp. 14392–14393, Jul. 2008.
[18] W. Fu, C. Nef, O. Knopfmacher, A. Tarasov, M. Weiss, M. Calame, and C. Schonenberger, "Graphene transistors are insensitive to pH changes in solution," *Nano Lett.*, vol. 11, pp. 3597–3600, Jul. 2011.
[19] Y. S. Chien, P. Y. Yang, W. L. Tsai, Y. R. Li, C. H. Chou, J. C. Chou, and H. C. Cheng, "The pH sensing characteristics of the extended-gate field-effect transistors of multi-walled carbon-nanotube thin film using low-temperature ultrasonic spray method," *J. Nanosci. Nanotechnol.*, vol. 12, pp. 5423–5428, Jul. 2012.
[20] R. S. Glaucio, Y. M. Elaine, C. Paola, M. R. Jose, and M. Marcelo, "Carbon felt/carbon nanotubes/pani as pH Sensor," *Mat. Res. Soc. Symp. Proc.*, vol. 1018, pp. 174–179, Jul. 2007.
[21] B. R. Huang and T. C. Lin, "Leaf-like carbon nanotube/nickel composite membrane extended-gate field-effect transistors as pH sensor," *Appl. Phys. Lett.*, vol. 99, pp. 023108-1–023108-3, Jul. 2011.
[22] Y. S. Chien, W. L. Tsai, I. C. Lee, J. C. Chou, and H. C. Cheng, "A novel pH sensor of extended-gate field-effect transistors with laser-irradiated carbon-nanotube network," *IEEE Electron Device Lett*, vol. 33, no. 11, pp. 1622–1624, Nov. 2012.
[23] Y. Miyamoto, A. Rubio, S. Berber, M. Yoon, and D. Tománek, "Spectroscopic characterization of Stone-Wales defects in nanotubes," *Phys. Rev. B*, vol. 69, pp. 121413-1–121413-4, Mar. 2004.
[24] T. I. T. Okpalugo, P. Papakonstantinou, H. Murphy, J. Mclaughlin, and N. M. D. Brown, "Oxidative functionalization of carbon nanotubes in atmospheric pressure filamentary dielectric barrier discharge," *Carbon*, vol. 43, pp. 2951–2959, Nov. 2005.
[25] M. J. Schoning, A. Simonis, C. Ruge, H. Ecken, M. M. Veggian, and H. Luth, "A bio-chemical field-effect sensor with macroporous Si as substrate material and a SiO_2/LPCVD-Si_3N_4 double layer as pH transducer," *Sensors*, vol. 2, pp. 11–22, Jan. 2002.
[26] S. Jamasb, S. Collins, and R. L. Smith, "A physical model for drift in pH ISFETs," *Sens. Actuators B*, vol. 49, pp. 146–155, Jun. 1998.
[27] J. C. Chou and C. W. Chen, "Long-term monitor of seawater by using TiO_2 :Ru sensing electrode for hard clam cultivation," *Int. J. Chem. Biol. Eng.*, vol. 2, pp. 176–180, 2009.
[28] Y. H. Liao and J. C. Chou, "Preparation and characteristics of ruthenium dioxide for pH array sensors with real-time measurement system," *Sens. Actuators B*, vol. 128, pp. 603–612, Jan. 2008.
[29] B. Peng, M. Locascio, P. Zapol, S. Li, S. L. Mielke, G. C. Schatz, and H. D. Espinosa, "Measurements of near-ultimate strength for multiwalled carbon nanotubes and irradiation-induced crosslinking improvements," *Nature Nanotechnol.*,, vol. 3, pp. 626–631, Aug. 2008.
[30] D. E. Yates, S. Levine, and T. W. Healey, "Site-binding model of the electrical double layer at the oxide/water interface," *J. Chem. Soc., Faraday Trans.*, vol. 70, pp. 1807–1818, Nov. 1973.
[31] S. M. Sze, *Physics of Semiconductor Device*, 2nd ed. New York, NY, USA: Wiley, 1981.
[32] R. E. G. van Hal, J. C. T. Eijkel, and P. Bergveld, "A novel description of ISFET sensitivity with the buffer capacity and double-layer capacitance as key parameters," *Sens. Actuator B*, vol. 24, pp. 201–205, 1995.
[33] P. Bruesch and T. Christen, "The electric double layer at a metal electrode in pure water," *J. Appl. Phys.*, vol. 95, pp. 2846–2856, Feb. 2004.

Wan-Lin Tsai received the B.S. degree in electronics engineering from National Chiao-Tung University, Hsinchu, Taiwan, in 2008. He is currently working toward the Ph.D. degree in the Department of Electronics Engineering, National Chiao-Tung University, Hsinchu, Taiwan.

His research interests include carbon nanotube and graphene in the applications of biosensor, field emission, and electronic devices.

Bai-Tao Huang received the B.S. degree from the Department of Physics, National Cheng Kung University, Tainan, Taiwan, in 2012. He is currently working toward the M.S. degree in the Department of Electronics Engineering, National Chiao-Tung University, Hsinchu, Taiwan.

His research interests include carbon nanotube and electronic devices.

Kuang-Yu Wang received the B.S. degree in materials science and engineering from National Tsing-Hua University, Hsinchu, Taiwan, in 2006. He is currently working toward the Ph.D. degree in the Department of Electronics Engineering, National Chiao-Tung University, Hsinchu, Taiwan.

His research interests include nanomaterials and biosensors.

Yu-Chih Huang received the B.S. degree from the Department of Electrophysics, National Chiao Tung University, Hsinchu, Taiwan, in 2008, where he is currently working toward the Ph.D. degree in the Department of Electronics Engineering, National Chiao Tung University, Hsinchu, Taiwan.

His current research interests include the areas of the thin-film-transistor (TFT) devices, metal oxide electronic components, resistive random- access memory (RRAM) devices, nanowire synthesis, and dielectric materials.

Po-Yu Yang received the B.S. degree from Institute of Display, National Chiao Tung University, Hsinchu, Taiwan, in 2007. He received the Ph.D. degree from the Department of Electronics Engineering, National Chiao-Tung University, Hsinchu, Taiwan, in 2011.

He is currently with the Taiwan Semiconductor Manufacturing Company, Hsinchu, Taiwan. His research interests include the applications of the devices with zinc-oxide-based nanostructures synthesized at low temperature.

Huang-Chung Cheng received the B.S. degree in physics from National Taiwan University in 1977, and the M.S. and Ph.D. degrees from the Department of Materials Science and Engineering, National Tsing-Hua University, Hsinchu, Taiwan, in 1979 and 1985, respectively.

He is currently a Professor in the Department of Electronics Engineering, National Chiao-Tung University, Hsinchu, Taiwan. He has published nearly 500 technical papers in international journals and conferences, and also held more than 50 patents. His current research interests include the areas of high-performance TFTs, novel nanowire devices, non-volatile memories, three-dimensional integrations, novel field emission displays, biosensors, and photoelectronic device.